East Tennessee State University

Digital Commons @ East Tennessee State University

5-2021

Synthesis of a Zinc Dipyrrin Complex for Photocatalytic Reduction of CO2

Sylvia Meredith

Follow this and additional works at: https://dc.etsu.edu/honors

Part of the Inorganic Chemistry Commons, and the Organic Chemistry Commons

Recommended Citation
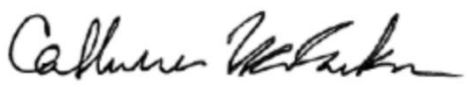
Synthesis of a Zinc Dipyrrin Complex for Photocatalytic Reduction of CO_2

By

Sylvia Meredith

An Undergraduate Thesis Submitted in Partial Fulfillment
of the Requirements for the
University Honors Scholars Program
Honors College
Department of Chemistry, East Tennessee State University

_____   5/5/21
Sylvia Meredith   Date

_____   5/5/21
Dr. Catherine McCusker, Thesis Mentor   Date

_____   5/5/21
Dr. Dane Scott, Reader   Date

<u>Abstract</u>

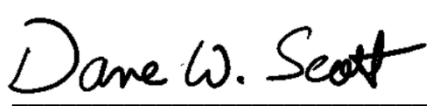Zinc dipyrrin complexes have the potential to act as cheap, effective photosensitizers. Synthesizing and studying different types could lead to more efficient solar energy harvesting processes, especially the production of solar fuel. Here, two attempts to synthesize 1,3,7,9-tetraphenyl-5-mesityldipyrromethene are reported and discussed. According to ^{1}H NMR, the first synthesis attempt was not successful. The second synthesis attempt was not purified effectively, so ^{1}H NMR produced inconclusive results. Further purification strategies or alternate synthesis methods are required.

<u>Acknowledgements</u>

I would like to thank my research professor, Dr. Catherine McCusker, for her mentorship during this research. Her clear explanations are particularly valuable to me and her involvement is extremely appreciated. It has been a high honor to work with her and to learn from her.

I would like to thank my reader Dr. Scott for his prompt and helpful feedback. I sincerely appreciate his willingness to invest in his students and I also look up to him greatly.

I would like to thank my fellow researcher Irene Dzaye for her guidance during lab work. Her cheerful advice is an excellent resource.

I would like to thank my whole family for their interest in my studies. It is easy to enjoy learning about science when supported and loved to such an extent.

Finally, I would like to thank the Lord for His faithfulness in all things. He has created a good world to learn about, and it has been my humble delight to study its chemistry.

Contents

<u>Background</u>

In 2019, 80% of the energy consumed by the United States came from fossil fuels. [1] Although the production of renewable energy reached an all-time high, the US still displayed a heavy reliance on coal, petroleum, and natural gas. In 2019, for example, the US burned 3.4 billion barrels of finished gasoline (140 billion gallons or 540 billion liters). [1,2] The reliance on fossil fuels is destructive to the environment: extraction accidents wreck local ecosystems, refining processes produce toxic waste, and burning fuel contributes to more than 75% of the country's total carbon emissions. [3] Negative impacts like these draw attention and value to green energy. Developing a cheap, clean, renewable source of fuel could effectively curtail some of the damaging effects of burning fossil fuels.

The development of renewable fuel sources can be inspired and informed by plants. Current solar panels produce electricity, but photosynthesis produces fuel, usually in the form of sugar. When the fuel is synthesized, it incorporates carbon dioxide that's already in the atmosphere, and when the fuel is burned, the CO_2 emissions reach a net zero. This fills many gaps in energy-related needs. Electricity, while useful, is not applicable in every circumstance. It cannot power an internal combustion engine, the dominant power supply for vehicles such as cars, boats, and airplanes. If photosynthesis could be copied and harnessed efficiently, more green fuel sources would be accessible to the general market and the applications of renewable energy would diversify.

The process of photocatalysis, the fundamental chemical reaction at the base of photosynthesis, has been extensively studied and has already been replicated in different ways. The easiest way to convert CO_2 to a usable liquid fuel is to reduce the compound to carbon monoxide (CO). [4] Through Fischer-Tropsch synthesis, CO and H_2 gas can be restructured into
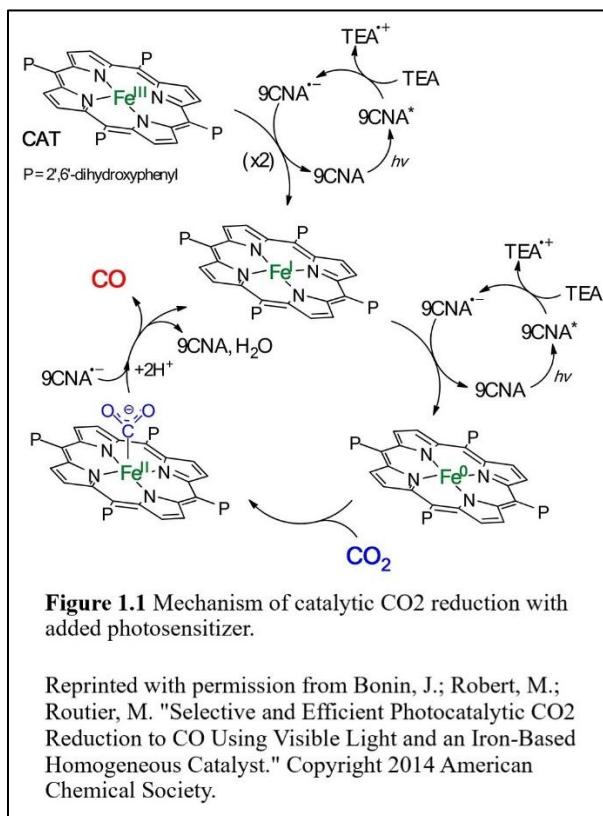
liquid gasoline. This mechanism relies on chain reactions—it is a widely studied and applicable technology. [5] When approaching the process of solar-generated fuel, it is extremely sensible to incorporate established processes like Fischer-Tropsch to simplify the aims in our own experimental designs.

The reduction of CO_2 relies on two primary components: a photosensitizer and a carbon dioxide reduction catalyst. A photosensitizer is a molecule which absorbs radiation (in this case, energy in the form of sunlight) and uses the energy to alter another molecule. [6] A carbon dioxide reduction catalyst is a compound that's specifically designed to add electrons to CO_2 and to instigate the transition to the more useful compound CO.

Some compounds, such as certain rhenium(I) diamine complexes (Re) can serve both functions. Re complexes are photochemically active and they can also selectively interact with carbon dioxide to form the desired CO. Although studying such rhenium complexes can provide great insight into the photocatalytic process as a whole, it's highly implausible to use them in the large-scale production of solar fuel. First, rhenium is rare and expensive. Second, the studied rhenium complexes denature relatively quickly. Catalysts occasionally bind to the CO_2 instead of reducing it, turning [*fac*-Re(bpy)(CO)$_3$Cl], for example, into [*fac*-Re(bpy)(CO)$_3$OC(O)H]. These resulting formate complexes no longer serve their purpose of reduction. Finally, rhenium complexes need to absorb lower wavelengths of light. They require ultraviolet light, rather than visible light, to operate efficiently, which increases their tendency to denature and requires more energy. [7] Sunlight only contains a small amount of ultraviolet light: only 5% of solar terrestrial radiation is between 100-400 nm. [8]

The limitations of Re complexes can be partially evaded when photocatalyzed carbon dioxide reduction processes incorporate separate components. Recent developments in carbon

dioxide reduction catalysts have produced a sizeable collection of effective and inexpensive

compounds that can act as co-catalysts for established photosensitizers. Iron porphyrin

complexes are a good example of such CO_2 reduction catalysts. These complexes have high

turnover numbers of carbon dioxide to carbon monoxide in photochemical processes. [9] When the

iron porphyrin complexes are paired with a photosensitizer, the speed and efficiency of carbon

dioxide reduction significantly increases, changing turnover numbers of 30 to turnover numbers

of up to 140. Photosensitizers absorb light in the visible region, rather than the ultraviolet region,

which means that they can catalyze a reduction reaction using a lower energy. This reduces the

photodegradation of the catalyst itself. The photosensitizer can also contribute the required

electron for C-O bond cleavage. [10] The electron transfer and the full reaction mechanism are both

pictured below in Figure 1.1, where 9-cyanoanthracene (9CNA) acts as a photosensitizer and

triethylamine (TEA) acts as the photosensitizer's electron donor.

Figure 1.1 Mechanism of catalytic CO2 reduction with added photosensitizer.

Reprinted with permission from Bonin, J.; Robert, M.; Routier, M. "Selective and Efficient Photocatalytic CO2 Reduction to CO Using Visible Light and an Iron-Based Homogeneous Catalyst." Copyright 2014 American Chemical Society.

In Figure 1.1, the changing oxidation state of the catalyst's central metal helps illustrate the path of electrons. The iron-carbon bond allows the reduction to take place, but the iron catalyst relies on the photosensitizer's solar-induced electron transfers.

The structures of iron porphyrin complexes have been well studied and well designed. Unfortunately, the most effective accompanying photosensitizers include the element iridium, which is rare and inaccessible like the previously mentioned rhenium. The cheapest accompanying photosensitizers, such as the 9-cyanoanthracene referenced in Figure 1, have low CO yields. To apply renewable fuel systems on a large scale, CO_2 reduction catalysts need photosensitizers that are both inexpensive and effective, unlike the options presented thus far.

In Figure 1.2, three examples of carbon dioxide reduction catalysts are pictured, including an iron porphyrin on the far left. All three of these complexes are built from inexpensive components and have successfully been paired with photosensitizers.

Figure 1.2 Three examples of carbon dioxide reduction catalysts
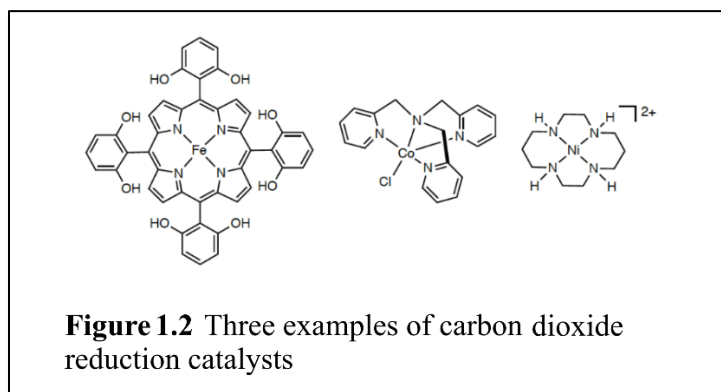
One of the aims of this research group is to develop novel photosensitizers which pair well with previously developed catalysts, specifically iron porphyrin complex catalysts. Zinc dipyrrin complexes have potential to serve such a purpose.

Why Zinc Dipyrrin complexes?

An ideal photosensitizer is cheap and easily made. It should absorb light and should effectively transfer an electron to a carbon dioxide reduction catalyst. In this context, this means the excited state of a photosensitizer must last long enough for electron transfer to occur. Zinc dipyrrin complexes fit all of the first requirements: they're not

Ground state   Singlet excited state   Triplet excited state

Figure 1.3 Visualization of electron spins in the ground state, singlet state, and triplet state
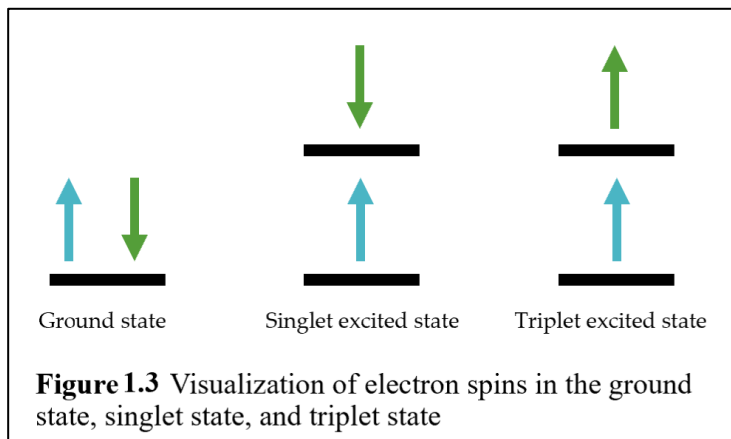
expensive or difficult to synthesize and they usually appear dark blue or purple. In certain conditions, these dipyrrin complexes have been observed to achieve long-lived triplet states. [11]

When valence electrons absorb energy, the electrons can be promoted to a higher orbital. "Spin up" and "spin down" describe the electrons' angular momentum. In Figure 1.3, the ground state energy is depicted on the far left. The two pictured electrons are occupying the same orbital and have different spins. The singlet excited state and triplet excited state both have electrons in different orbitals, but the triplet excited state energy contains electrons which also have the same spin. A triplet state is difficult to achieve, but since the de-excitation state is spin-forbidden, it will last a long time.

A zinc dipyrrin complex's properties change based on the structures of its ligands. Such structures are easily manipulated. When symmetrical ligands include a central mesityl group (as opposed to phenyl) the lifetimes of singlet excited states in zinc dipyrrin complexes significantly increase. Most bis(dipyrrinato)-metal complexes are not able to retain their excited states for long periods of time, which makes this aspect of zinc complexes stand out. [12]

Figure 1.4 Visualization of the central mesityl groups on a zinc dipyrrin complex
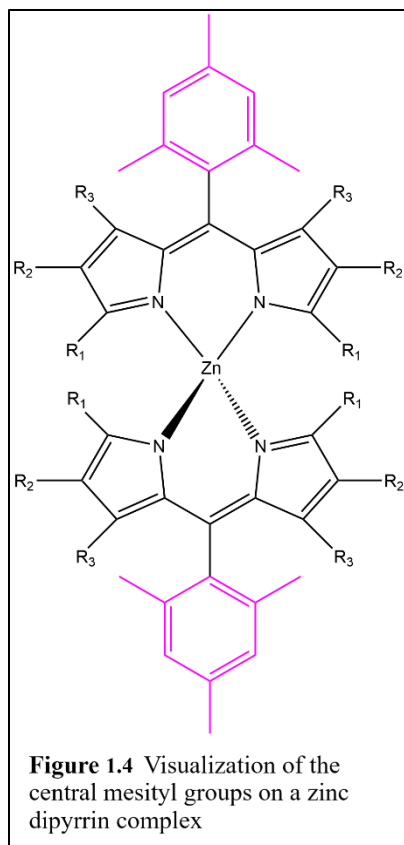
A visualization of such mesityl groups are pictured in pink in Figure 1.4. Mesityl groups contribute more steric hinderance, reducing the likelihood that a complex can spend its energy on conformational changes. The symmetry in zinc dipyrrin complexes is illustrated as well in Figure 1.4. Two identical ligands are attached orthogonally to a central zinc ion. In polar solvents, symmetrical complexes (such as these) lose their symmetry when an electron on one ligand is transferred to the other. The ligand accepting the electron becomes negatively charged, and the other ligand becomes positively charged. Theoretically, this symmetry-breaking charge-transfer encourages intersystem crossing, or quick transitions between electronic states with different spin multiplicities (such as the transition from a singlet state to a triplet state). Efficient formations of charge-separated states do not necessarily increase the formations of triplet states, but the long-lasting triplet states have been quantified and observed in zinc complexes which display these tendencies. [11] [13]

The effects of mesityl groups are already established, but the effects of different functional groups at the R1, R2, and R3 positions in Fig 1.3 have not been studied in detail. If photosensitizers are to be developed from zinc dipyrrin complexes, it is important to understand how these R groups contribute to the complex's properties. The groups may affect how the complex interacts with light, how well it can form and maintain triplet excited states, and how effectively it interacts with carbon dioxide reduction catalysts. For a photosensitizer to react well with an accompanying catalyst, the photosensitizer's reduction potential must be higher than the

reduction potential of the catalyst itself. [14] Zinc dipyrrin complexes do have higher reduction potentials than the iron porphyrin complex 5,10,15,20-tetrakis(pentafluorophenyl)-21H,23Hporphyriniron(III) chloride, and have been successfully paired with that catalyst to reduce carbon dioxide. [15]

A previous study by this lab group compared the formation of triplet excited states between two zinc dipyrrin complexes. Both complexes produced triplet state yields were significantly higher than the triplet state yields of photosensitizers like 9-cyanoanthracene. The functional groups of the two complexes were very similar: both had methyl groups on R1 and R3. The first compound, which had a hydrogen at R2, did not form triplet states as efficiently as the complex with an iodine at R2. [13] The effects of other functional groups, such as aromatic functional groups, are still unknown, but such knowledge could be highly useful in the optimization of a zinc dipyrrin photosensitizer. The goal of this experiment was to substitute a phenyl ring at the R1 and R3 positions (with a hydrogen at R2). Since aromatic groups are extremely bulky, the resulting zinc dipyrrin complex would be much more rigid. The absorption from phenol rings may increase the amount of sunlight that the complex is able to absorb or change the complex's absorption maximum wavelength.

Experimental Methods

General Procedure

All solvent and reagents were used as received, unless otherwise specified. NMR data was collected using a 400 MHz JEOL AS400 FT-NMR spectrometer and processed using SpinWorks 4.2.10 software. The starting compound 2,4-diphenyl-1H-pyrrole was synthesized according to published procedures. [16] The two attempted syntheses of 1,3,7,9-tetraphenyl-5-mesityldipyrromethene were performed according to modified literature procedures. [11, 17] The two procedures are described below.

Synthesis A [11]

2,4-dipheynl-1H-pyrrole (0.5 g, 2.28 mmols) and mesitaldehyde (0.46 mL, 10.40 mmols) was added to 20 mL dichloromethane under nitrogen. When pyrrole had dissolved, 2 drops trifluoroacetic acid was added to the solution and the reaction was stirred under nitrogen for 6 hours. The reaction was quenched with 3 drops triethylamine, washed three times with 10 mL DI water, and washed once with 15 mL brine (a saturated solution of NaCl in water). The product was dried with anhydrous Na_2SO_4 and the solvent was removed under reduced pressure.

The ligand product was added to 25 mL freshly distilled THF under nitrogen. When the ligand had dissolved, 2,3-dichloro-5,6-dicyano-p-benzoquinone (0.703 g, 3.10 mmols) in 4 mL THF was added and the reaction was stirred under nitrogen for 1 hour. The reaction was quenched with 1 mL triethylamine, washed five times with 10 mL of saturated sodium bicarbonate, and washed once with 15 mL brine. The product was dried with anhydrous Na_2SO_4
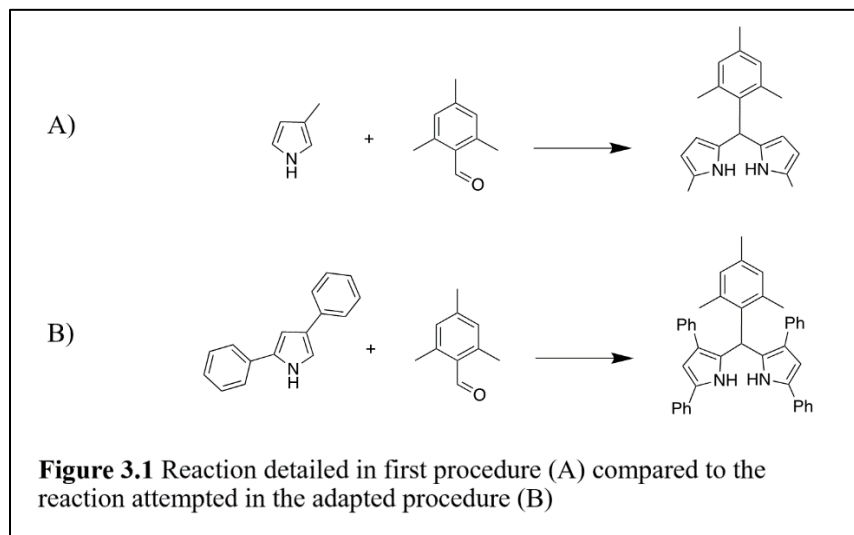
and the solvent was removed under reduced pressure. The final product was purified through

column chromatography. Alumina, 4", was used with a dichloromethane solvent.

Synthesis B [17]

2,4-diphenyl-1H-pyrrole (0.30 g, 1.37 mmols) and trimethylbenzoic acid (0.13g, 0.79

mmols) was dissolved in 5 mL phosphorous oxychloride. The solution was kept over steam for

one hour, cooled to room temperature, then poured over ice (~100-50 mL). Phosphorous

oxychloride reacts vigorously with water and can cause a solution to boil if not chilled to the

appropriate extent. When the phosphorous oxychloride had finished reacting with water, the

solution was heated to boiling. The solvent was cooled and poured off of the tar-like product,

then the tar was rinsed once with ~20 mL water. Methanol was added dropwise to the tar until

the product had fully dissolved, then the methanol and product was poured into 100 mL of 0.1M

NaOH. The resulting precipitate was filtered and dried in a desiccator. The final product was

purified through column chromatography. 6" of alumina was used with a 40/60

dichloromethane/hexanes solvent mixture.

Results and Discussion

Two different synthesis procedures were used, with the aim of creating the ligand 1,3,7,9-tetraphenyl-5-mesityldipyrromethene. The first attempt was based on the procedure detailed in "Symmetry-Breaking Charge Transfer of Visible Light Absorbing Systems: Zinc Dipyrrins" by Trinh et al. [11] The procedure was followed with one adaptation to the starting compounds: instead of the 2-methylpyrrole, the 2,4-diphenyl-1H-pyrrole was used. The two reactions are compared in Figure 3.1 to highlight the differences in pyrrole structure.

Figure 3.1 Reaction detailed in first procedure (A) compared to the reaction attempted in the adapted procedure (B)

To identify whether or not the target ligand had been synthesized, the product was measured through proton nuclear magnetic resonance spectroscopy (^{1}H NMR). ^{1}H NMR is a useful tool for the identification of organic complexes because it is able to provide detailed information on a molecule's structure. An ^{1}H NMR's magnetic field will affect each proton in a slightly different way, based on that proton's local chemical environment. [18]

To determine the success or failure of the synthesis, an expected set of ^{1}H NMR peaks were compiled. They were pulled from two sources: previous literature of the ^{1}H NMR spectra of

the two starting compounds, and the chemical structure of the final ligand product. The ^{1}H NMR

spectrum of 2,4-diphenyl-1H-pyrrole is depicted below in Figure 3.2.

Figure 3.2 Structure and 'H NMR spectra of 2,4-diphenyl-1H-pyrrole
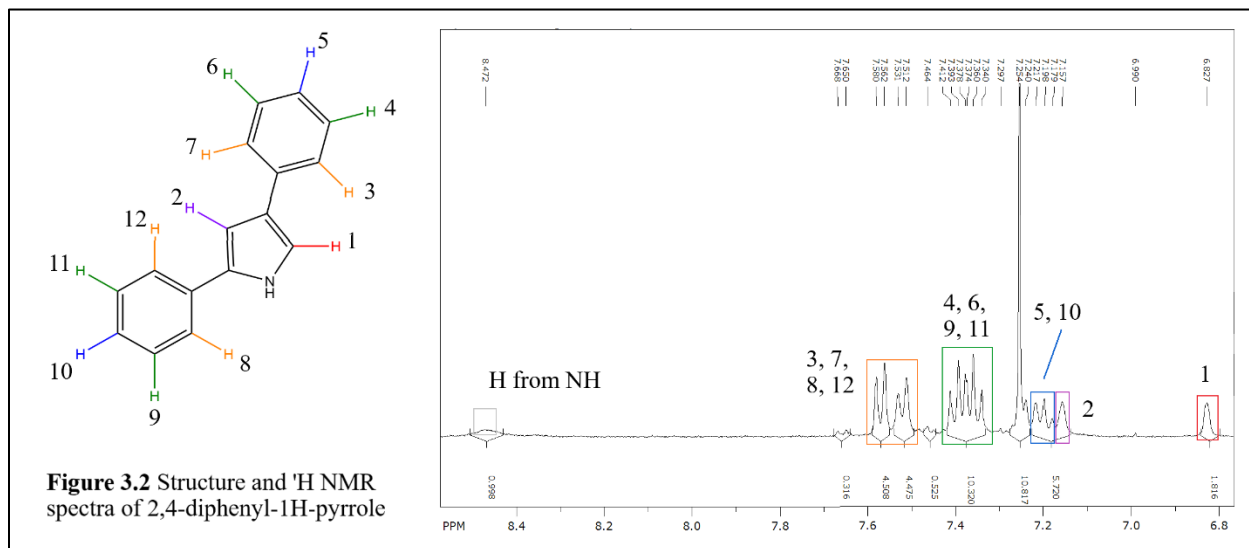
The hydrogens here are colored and labeled to ensure clarity. This spectrum was acquired

from the 2,4-diphenyl-1H-pyrrole which had been synthesized in lab. All shifts present here are

in accordance with recorded NMR values [16] which are printed below

in Table 3.1.

When the pyrrole in Figure 3.2 is converted to the target

ligand, which is illustrated in Figure 3.3, hydrogen 1 (marked in red)

is no longer part of the structure. The peak at 6.8 ppm should not be

present in the ^{1}H NMR of 1,3,7,9-tetraphenyl-5-

mesityldipyrromethene.

Figure 3.3
1,3,7,9-tetraphenyl-5-
mesitaldehyde
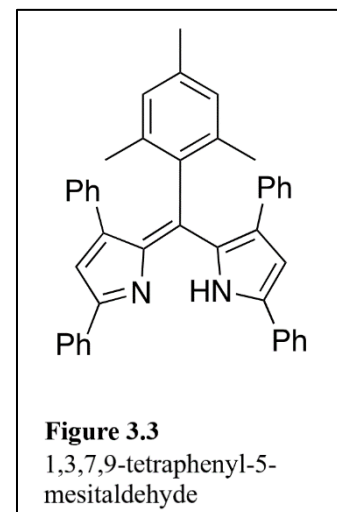
The conversion of 2,4-diphenyl-1H-pyrrole and mesitaldehyde to the target ligand can

change the ^{1}H NMR peaks in other ways as well. First, they could change by location. Peaks that

were originally found around 7.6 ppm could shift upfield or downfield due to their new local

chemical environment. Second, the peaks could change in size and group. Hydrogens 3, 7, 8, and 12 are grouped together in Figure 3.2, but a ligand could reduce the symmetry between them and increase the number of distinct ^{1}H NMR signals. When the synthesis procedure had been completed, the product was separated through column chromatography and consolidated into three fractions. The recorded ^{1}H NMR peaks of mesitaldehyde in CDCl$_3$ were combined with the ^{1}H NMR peaks of the pyrrole to produce a set of expected peaks for the ligand. These are printed in Table 3.1

Table 3.1 ^{1}H NMR signals of reagents and projected products in CDCl$_3$

| 2,4-diphenyl-1H-pyrrole	mesitaldehyde	ligand (projected)
8.45 (bs, 1H)	10.515 (s, 2H)	8.45 (bs, 1H)
7.5-7.58 (m, 4H)	7.1 (d, 2H)	7.5-7.58 (m, 4H)
7.34-7.42 (m, 4H)	2.36 (s, 6H)	7.34-7.42 (m, 4H)
7.17-7.27 (m, 2H)	2.31 (s, 3H)	7.17-7.27 (m, 2H)
7.15 (d, 1H)		7.15 (d, 1H)
6.83 (d, 1H)		7.1 (d, 2H)
		2.36 (s, 6H)
		2.31 (s, 3H)

Unfortunately, the three collected fractions did not show signals indicative of formed ligands. The observed peaks are listed below in Table 3.2.

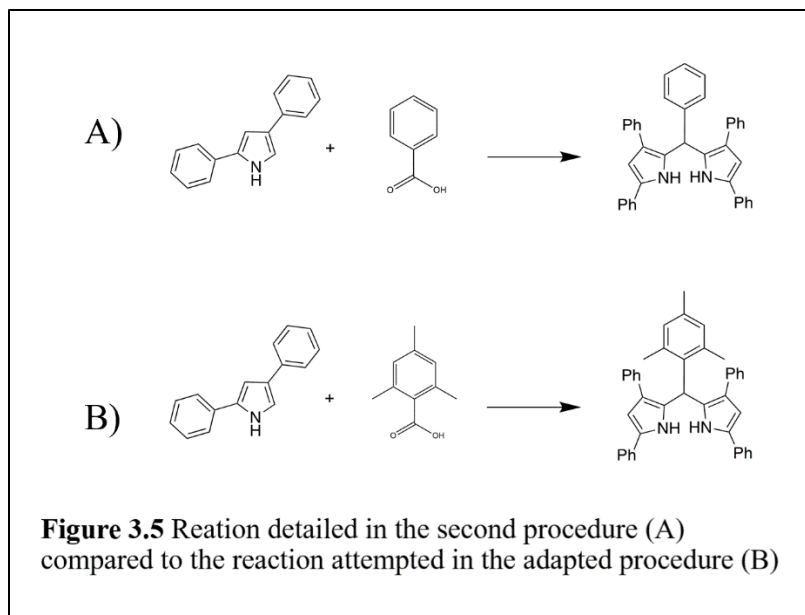**Table 3.2** ^{1}H NMR signals of first synthesis attempt

Fraction 1	Fraction 2	Fraction 3
	10.56 (s)	
7.92 (s)	7.93 (s)	7.93 (s)
7.51 (s)	7.219 (d)	7.51 (s)
6.99 (d)	6.903 (s)	6.99 (s)
5.3 (s)		5.3 (s)
3.74 (m)	3.746 (m)	3.74 (m)
	2.583 (s)	

Fraction 3 is presented below in Figure 3.4 as an example ^{1}H NMR. Several peaks are present here, including two peaks near 2.4 ppm which are expected from the mesityl group. Unfortunately, the aromatic region is fairly empty. The characteristic peak clusters produced by the phenyl groups are not evident, so the final ligand is definitely not present.

An interesting observation here is that several of the signals are present in all 3 fractions, such as the signal at 6.9 ppm. These ^{1}H NMR measurements were taken alongside a measurement of the plain $CDCl_3$ solvent, so the peaks recorded in Table 3.2 do not include any impurities from the solvent.

Figure 3.4 'H NMR of second chromatography fraction, first synthesis attempt
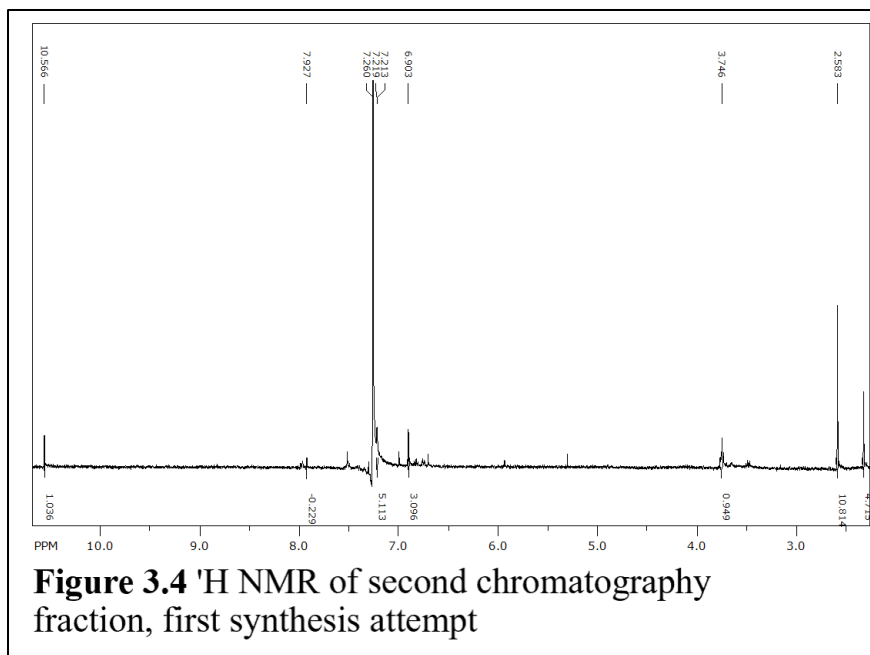
Ultimately, this was not a successful synthesis. None of the collected fractions showed peaks congruent with expectations. Because of this, the second synthesis procedure, based on a paper by Rogers (1943), [17] was attempted on a large enough scale for similar purification. This procedure was different because the chosen synthesis procedure included pyrroles with phenyl groups. Modifications were made to the second reagent instead: methylbenzoic acid was substituted for benzoic acid. The two reactions are compared below in Figure 3.5.

Figure 3.5 Reation detailed in the second procedure (A) compared to the reaction attempted in the adapted procedure (B)

The products were separated through column chromatography. The separation produced seven distinct visual layers, but when the layers were compared via thin layer chromatography, the initial distinct colors were consolidated into three. All three final fractions appeared in various shades of pink and magenta.

The column itself is pictured in Figure 3.6. Here, five layers are visible: yellow, peach, purple, green, and light blue.

The three condensed fractions were measured via ^{1}H NMR. The shift values of each fraction are recorded below in Table 3.3.
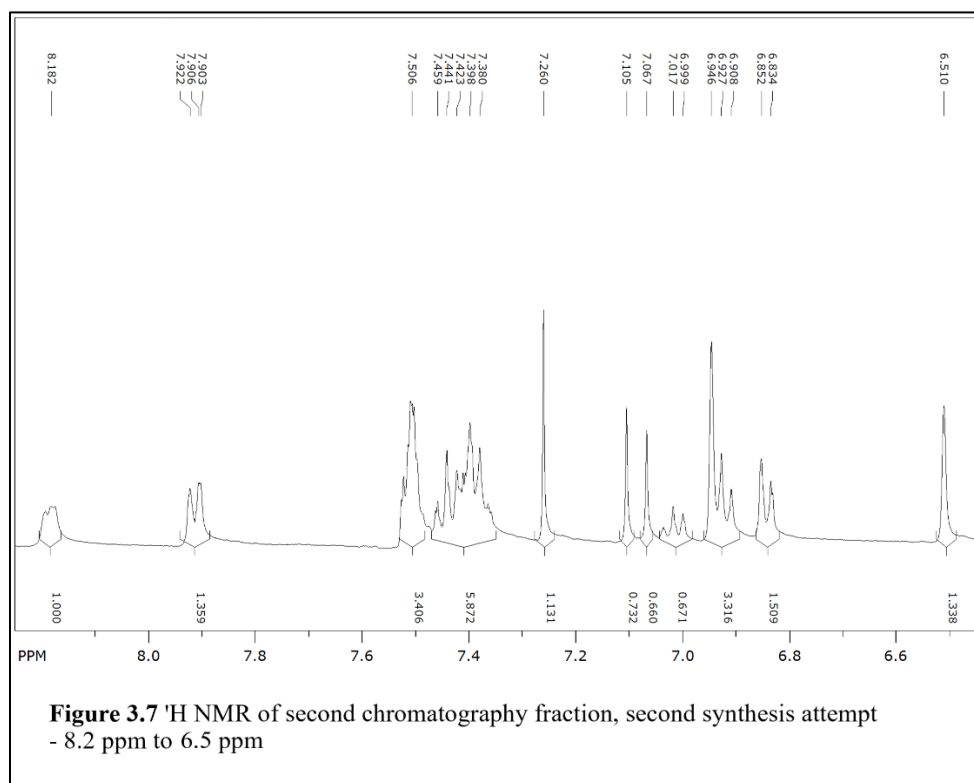

Figure 3.6 Photograph of the column chromatography process for the purification of the 2nd synthesis procedure

Table 3.3 ^{1}H NMR signals of second synthesis attempt

Fraction 1	Fraction 2	Fraction 3
8.45 (d)	8.18 (bs, 2H)	8.45 (d)
7.98 (d, 2H)	7.91 (d, 2H)	7.97 (d)
7.645 (d, 3H)	7.45 (m, 6H)	7.65 (d)
7.527 (m, 6H)	7.38 (m, 10H)	7.54 (m, 4H)
7.467 (m, 10H)		7.45 (m, 4H)
7.366 (m, 7H)	7.11 (s, 2H)	7.37 (m, 3H)
7.242 (m, 1H)	7.06 (s, 1H)	7.24 (m, 2H)
7.043 (m, 1H)	7.01 (m, 1H)	7.03 (s, 1H)
6.96 (s, 3H)	6.99 (t, 5H)	6.99 (d, 1H)
6.824 (s)	6.8 (d, 3H)	6.743 (m)
6.76 (d)	6.5 (s, 2H)	6.703 (m)
6.703 (s)		6.588 (d, 1H)
6.588 (bs, 2H)		6.494 (bs, 1H)
6.5 (bs, 3H)		
	2.343 (s, 4H)	
	2.296 (s, 9H)	
2.117 (bs, 1H)	2.177 (s, 7H)	2.124 (s)
2.072 (bs, 2H)	2.099 (s, 4H)	2.078 (s)
1.694 (bs, 7H)	1.764 (bs, 7H)	1.970 (s)
1.415 (s)	1.252 (m)	1.676 (bs)
1.273 (m, 10H)	0.882 (m)	1.248 (s)
0.964 (d, 1H)		0.879 (m)
0.839 (m, 10H)		

As evident by the table alone, the ^{1}H NMR samples were very impure even after the sample was separated into fractions. This suggests that the stationary and mobile phase that were

used in the column could not effectively separate the primary product from the rest of the compounds in the mixture.

When Table 3.3 is compared to the projected ligand values in Table 3.1, there are certainly clear overlaps. Fraction 2 has two peaks near 2.3 ppm, which match the expected peaks from the mesityl group. All three fractions showed strong signals in the aromatic region, and shared many peaks with the starting pyrrole. Unfortunately, the sheer quantity of peaks in each layer prevents definite conclusions from being drawn. Nevertheless, Figures 3.7 and 3.8 are presented below of the ^{1}H NMR spectrum of Fraction 2, to discuss speculations with more ease.

Figure 3.7 ^{1}H NMR of second chromatography fraction, second synthesis attempt - 8.2 ppm to 6.5 ppm

In Figure 3.7, the aromatic region is presented alone to increase the visibility of individual peaks. There are clear similarities here to the peaks in Figure 3.2, but it is easy to visualize how much noise and interference is caused by the presence of impurities. The final

ligand could certainly have been formed, since no major peaks here are found to be missing. The
second chromatography layer is most likely to contain it, since this layer includes the peaks at
2.3 ppm which can be seen in Figure 3.8.

Figure 3.8 should contain only contain two peaks when measuring the ligand alone. Here,
seven are visible. Some of the peaks might come from solvents which were used in the synthesis
or used in the chromatography purification process. The broad peak at 1.7 ppm, for example,
might come from atmospheric water, which usually appears around 1.56 ppm. [19]

Figure 3.8 'H NMR of second chromatography fraction, second synthesis attempt - 2.4 ppm to 0.6 ppm
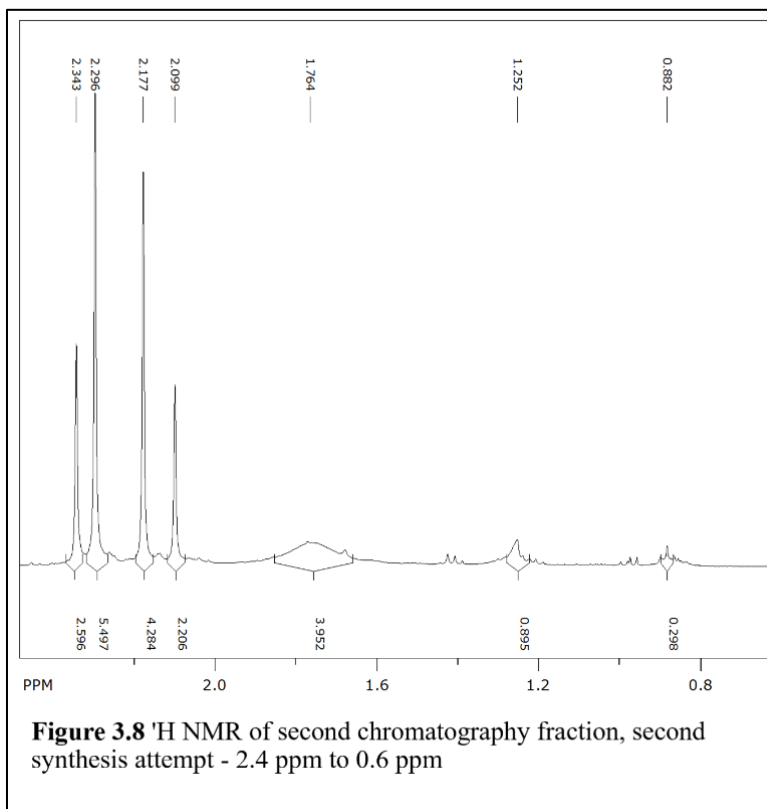
<u>Conclusions</u>

Because the final fractions were full of impurities, no definite conclusions could be drawn about the synthesis's success. There were peaks in expected regions, but there were also several other peaks.

The difficulties in purification might be attributed to the nitrogens present in the finished ligand. These nitrogens would ensure rapid bonding when the ligand is introduced to zinc ions, but their reactivity could hinder their movement in a column. Their reactivity could also cause interactions with impurities and complicate other attempts at purification.

One way to combat this would be to introduce the speculated ligand to a solution of zinc ions, similar to the procedure detailed in Trinh et al (2014) for the formation of zinc dipyrrin complexes. If the ligand is able to form a complex with zinc, even in the presence of impurities, the final zinc product might be separated and characterized more easily than the individual ligand. [11] Another beneficial approach could be the further optimization of ligand purification techniques. Column chromatography fractions might become more distinct with a different combination of solvents.

References:

(1)   U.S. energy facts explained - consumption and production - U.S. Energy Information Administration (EIA) https://www.eia.gov/energyexplained/us-energy-facts/ (accessed Feb 18, 2021).

(2)   Supply and Disposition of Crude Oil and Petroleum Products https://www.eia.gov/dnav/pet/pet_sum_snd_d_nus_mbbl_a_cur.htm (accessed Feb 18, 2021).

(3)   Where greenhouse gases come from - U.S. Energy Information Administration (EIA) https://www.eia.gov/energyexplained/energy-and-the-environment/where-greenhouse-gases-come-from.php (accessed Feb 18, 2021).

(4)   Benson, E. E.; Kubiak, C. P.; Sathrum, A. J.; Smieja, J. M. Electrocatalytic and Homogeneous Approaches to Conversion of CO2 to Liquid Fuels. *Chem Soc Rev* **2009**, *38* (1), 89–99. https://doi.org/10.1039/B804323J.

(5)   Davis, B. H. Fischer–Tropsch Synthesis: Current Mechanism and Futuristic Needs. *Fuel Process. Technol.* **2001**, *71* (1), 157–166. https://doi.org/10.1016/S0378-3820(01)00144-8.

(6)   IUPAC - photosensitization (P04652) https://goldbook.iupac.org/terms/view/P04652 (accessed Feb 18, 2021). https://doi.org/10.1351/goldbook.P04652.

(7)   Hori, H.; Takano, Y.; Koike, K.; Sasaki, Y. Efficient Rhenium-Catalyzed Photochemical Carbon Dioxide Reduction under High Pressure. *Inorg. Chem. Commun.* **2003**, *6* (3), 300–303. https://doi.org/10.1016/S1387-7003(02)00758-X.

(8)   International Agency for Research on Cancer. Solar and Ultraviolet Radiation. **2012**, No. 100D.

(9)   Bonin, Julien; Chaussemier, Marie; Robert, Marc; Routier, Mathilde. Homogeneous Photocatalytic Reduction of CO2 to CO Using Iron(0) Porphyrin Catalysts: Mechanism and Intrinsic Limitations. *Eur. Soc. J. Catal.* **2014**, No. 6.11, 3200–3207.

(10) Bonin, J.; Robert, M.; Routier, M. Selective and Efficient Photocatalytic CO2 Reduction to CO Using Visible Light and an Iron-Based Homogeneous Catalyst. *J. Am. Chem. Soc.* **2014**, *136* (48), 16768–16771. https://doi.org/10.1021/ja510290t.

(11) Trinh, C.; Kirlikovali, K.; Das, S.; Ener, M. E.; Gray, H. B.; Djurovich, P.; Bradforth, S. E.; Thompson, M. E. Symmetry-Breaking Charge Transfer of Visible Light Absorbing Systems: Zinc Dipyrrins. *J. Phys. Chem. C* **2014**, *118* (38), 21834–21845. https://doi.org/10.1021/jp506855t.

(12) Sazanovich, I. V.; Kirmaier, C.; Hindin, E.; Yu, L.; Bocian, D. F.; Lindsey, J. S.; Holten, D. Structural Control of the Excited-State Dynamics of Bis(Dipyrrinato)Zinc Complexes: Self-Assembling Chromophores for Light-Harvesting Architectures. *J. Am. Chem. Soc.* **2004**, *126* (9), 2664–2665. https://doi.org/10.1021/ja038763k.

(13) Alqahtani, N. Z.; Blevins, T. G.; McCusker, C. E. Quantifying Triplet State Formation in Zinc Dipyrrin Complexes. *J. Phys. Chem. A* **2019**, *123* (46), 10011–10018. https://doi.org/10.1021/acs.jpca.9b08682.

(14) Azcarate, I.; Costentin, C.; Robert, M.; Savéant, J.-M. Dissection of Electronic Substituent Effects in Multielectron–Multistep Molecular Catalysis. Electrochemical CO2-to-CO Conversion Catalyzed by Iron Porphyrins. *J. Phys. Chem. C* **2016**, *120* (51), 28951–28960. https://doi.org/10.1021/acs.jpcc.6b09947.

(15) Rasheed, S. Photocatalytic Carbon Dioxide Reduction with Zinc(II) Dipyrrin Photosensitizers and Iron Catalyst. Masters, East Tennessee State University, 2020.

(16)   Hall, M. J.; McDonnell, S. O.; Killoran, J.; O'Shea, D. F. A Modular Synthesis of
        Unsymmetrical Tetraarylazadipyrromethenes. *J. Org. Chem.* **2005**, *70* (14), 5571–5578.
        https://doi.org/10.1021/jo050696k.
(17)   Rogers, M. A. T. 4-Diarylpyrroles. Part II. Methines. *J. Chem. Soc. Resumed* **1943**, No. 0,
        596–597. https://doi.org/10.1039/JR9430000596.
(18)   Robert M. Granger II; Hank M. Yochum; Jill N. Granger; Karl D. Sienerth. *Instrumental
        Analysis*; Oxford University Press: New York, NY, 2017.
(19)   Fulmer, G. R.; Miller, A. J. M.; Sherden, N. H.; Gottlieb, H. E.; Nudelman, A.; Stoltz, B.
        M.; Bercaw, J. E.; Goldberg, K. I. NMR Chemical Shifts of Trace Impurities: Common
        Laboratory Solvents, Organics, and Gases in Deuterated Solvents Relevant to the
        Organometallic Chemist. *Organometallics* **2010**, *29* (9), 2176–2179.
        https://doi.org/10.1021/om100106e.